Articles

Ligand Binding to the Tissue-Type Plasminogen Activator Kringle 2 Domain: Structural Characterization by ^{1}H-NMR†

In-Ja L. Byeon,‡ Robert F. Kelley,§ Michael G. Mulkerrin,§ Seong Soo A. An,‡ and Miguel Llinás*,‡

Department of Chemistry, Carnegie Mellon University, Pittsburgh, Pennsylvania 15213, and Protein Engineering Department, Genentech, Inc., South San Francisco, California 94080

Received July 18, 1994; Revised Manuscript Received October 18, 1994⊗

ABSTRACT: Ligand binding to a recombinant human tissue-type plasminogen (tPA) kringle 2 domain has been characterized via ^{1}H-NMR spectroscopy at 500 MHz. Seven ω-amino acid ligands were investigated: L-Lys, 6-aminohexanoic acid (6AHA), 7-aminoheptanoic acid (7AHA), *trans*-(aminomethyl)-cyclohexanecarboxylic acid (AMCHA), *p*-(aminomethyl)benzoic acid (PAMBA), *p*-(aminoethyl)benzoic acid (PAEBA), and *p*-benzylaminesulfonic acid (BASA). The interactions with two peptides containing a C-terminal lysyl residue, Tyr-Leu-Leu-Lys (YLLK) and Ala-Phe-Gln-Tyr-His-Ser-Lys (AFQYHSK), were also studied. The sequence AFQYHSK is found within the plasminogen N-terminal activation peptide while the tetrapeptide YLLK corresponds the 119−122 segment of the fibrinogen Bβ-chain. Spectral comparison of ligand-free and ligand-containing kringle 2 samples leads to the conclusion that all the small ligands as well as the peptides' C-terminal lysyl residues interact with a common binding site in kringle 2. Two-dimensional spectra show that besides the Tyr^{36}, Trp^{62}, His^{64}, Trp^{72}, and Tyr^{74} aromatic rings, the Val^{35} and Asp^{55} aliphatic side chains also participate in ligand binding. Contact points with the ligands 6AHA and BASA were unambiguously identified from kringle 2−ligand nuclear Overhauser effects (NOEs). Overall, the ligand-induced chemical shifts and the intermolecular NOEs correlate remarkably well. Association constant (K_a) values for the kringle 2−ligand interactions were determined. Among the investigated ligands, BASA perturbs the kringle 2 spectrum the most and exhibits the highest affinity for kringle 2 ($K_a \sim 233$ mM^{-1}). Of the two other aromatic ligands, PAEBA binds to kringle 2 less firmly ($K_a = \sim 12$ mM^{-1}) than does the one-methylene group shorter analog PAMBA ($K_a \sim 31$ mM^{-1}). By comparison, relative to 6AHA ($K_a \sim 22$ mM^{-1}), the longer chain linear aliphatic ligand 7AHA interacts with kringle 2 with significantly higher affinity ($K_a \sim 149$ mM^{-1}). By reference to the NMR-derived binding site structure, it is suggested that the higher affinity toward 7AHA may stem from (a) a relatively more favored ionic pairing between its carboxylate group and the Lys^{34} + Arg^{69} side-chain cationic centers and (b) an enhanced interaction between the ligand hydrocarbon moiety and the kringle hydrophobic pocket, in particular with the Leu^{70} side chain. The latter is consistent with the relatively good affinity of kringle 2 for the cyclic hydrocarbon ligand AMCHA ($K_a \sim 69$ mM^{-1}). When compared against L-Lys ($K_a \sim 18$ mM^{-1}), the higher affinity exhibited by YLLK and AFQYHSK ($K_a \sim 38$ mM^{-1}) indicates that the attached polypeptide chain segments contribute positively to their binding to kringle 2. Overall, the NMR ligand-binding data are in harmony with the binding site structure, solvent accessibility, and pH sensitivity of individual residues and confirm, as found for other kringles, that the ligand complexation event is not accompanied by any significant conformational change of the kringle fold.

As is the case for the plasminogen kringle 1 (Pgn/K1),[1] K2, K4, and K5 domains (Lerch *et al.*, 1980; Winn *et al.*, 1980; Hochschwender *et al.*, 1983; Váli & Patthy, 1984; De Marco *et al.*, 1986; Thewes *et al.*, 1990; Marti *et al.*, 1994), the tissue plasminogen activator (tPA) K2 module exhibits binding affinity for L-lysine and for zwitterionic ω-amino acid analogs of similar molecular size (van Zonneveld *et al.*, 1986a,b; Cleary *et al.*, 1989; Byeon *et al.*, 1989). Thus, in conjunction with the finger domain, the second kringle has been proposed to mediate tPA fibrin binding through interactions with lysyl side chains exposed by the fibrin matrix within the blood clot (van Zonneveld *et al.*, 1986b;

† This research was supported by the U.S. Public Health Service, NIH Grant HL 29409, and Genentech, Inc. Support from the Pittsburgh Supercomputing Center through the NIH Division of Research, Cooperative Agreement U41RR04154, is gratefully acknowledged.

‡ Carnegie Mellon University.

§ Genentech, Inc.

⊗ Abstract published in *Advance ACS Abstracts,* January 15, 1995.

[1] Abbreviations: AFQYHSK, Ala-Phe-Gln-Tyr-His-Ser-Lys; 6AHA, 6-aminohexanoic acid; 7AHA, 7-aminoheptanoic acid; AMCHA, *trans*-(aminomethyl)cyclohexanecarboxylic acid; BASA, *p*-benzylamine-sulfonic acid; COSY, two-dimensional chemical shift correlated spectroscopy; K_a, ligand−kringle equilibrium association constant; K1, kringle 1; K2, kringle 2; K3, kringle 3; K4, kringle 4; K5, kringle 5; NOE, nuclear Overhauser effect; NOESY, two-dimensional NOE correlated spectroscopy; PAEBA, *p*-(aminoethyl)benzoic acid; PAMBA, *p*-(aminomethyl)benzoic acid; Pgn, plasminogen; pH*, glass electrode pH reading uncorrected for deuterium isotope effects; Ptb, prothrombin;

0006-2960/95/0434-2739$09.00/0

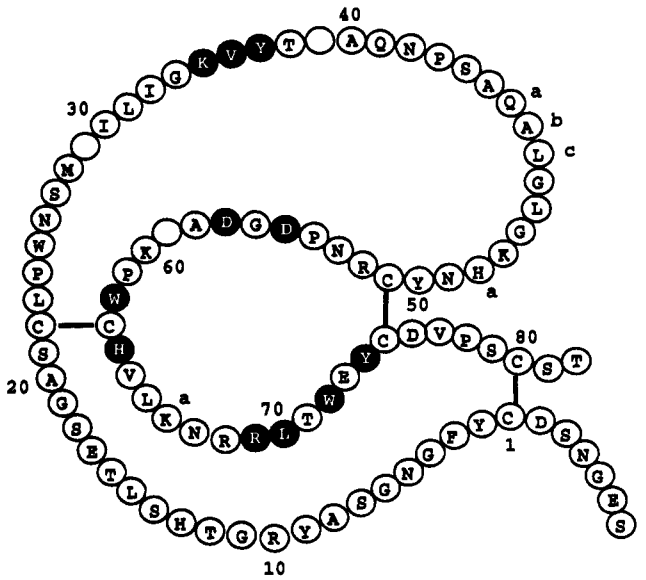

FIGURE 1: Recombinant kringle 2 of human tPA: sequence outline. Reverse, white-on-black print identify residues which contribute to structuring the ligand binding site and are discussed in the text. Residue numbering is as in previous papers (Byeon *et al.*, 1989, 1991). Insertions and deletions relative to homologous kringles (Tulinsky *et al.*, 1988) are labeled with lower-case letters (a, b, c) or indicated by a blank area, respectively.

Verheijen *et al.*, 1986; Gething *et al.*, 1988; Horrevoets *et al.*, 1994). Indeed, a tPA domain-deletion mutant containing only the K2 and protease domains retains much of the fibrin-binding specificity associated to intact tPA (Pannekoek *et al.*, 1990; Kohnert *et al.*, 1992). However, despite the functional similarity to the Pgn kringles, the tPA/K2 domain distinguishes itself structurally in that (a) its primary sequence contains a three-residue insertion between sites 44 and 45 and single-residue insertions between sites 48 and 49 and between sites 66 and 67 (Figure 1) and (b) its secondary structure exhibits a six-residue α-helix comprising residues Ser^{43} through Gly^{45} (Byeon *et al.*, 1991; de Vos *et al.*, 1992). Hence, it is not surprising that the two types of kringles differ, qualitatively as well as quantitatively, in their small ligand specificities (Thewes *et al.*, 1990; Kelley *et al.*, 1991; Rejante *et al.*, 1991b), a factor which may be of consequence in their interactions with fibrin(ogen) (Rejante *et al.*, 1991a; Horrevoets *et al.*, 1994).

Elsewhere, we have reported a ^{1}H-NMR characterization of a recombinant tPA/K2 module complexed to 6AHA, a lysine analog (Byeon *et al.*, 1989, 1991). In a parallel study, the crystallographic structure of the ligand-free K2 was determined (de Vos *et al.*, 1992) and shown to be in excellent overall agreement with the solution conformation of the 6AHA complex (Byeon & Llinás, 1991). In this paper we report a detailed ^{1}H-NMR study of ligand binding to the tPA/K2. The interactions of the kringle with L-Lys and with a number of related ω-amino acid analogs were investigated. The tested compounds include a series of antifibrinolytic drugs (Skoza *et al.*, 1968; Markwardt, 1978) and are well-characterized ligands of the Pgn kringles. They are (Chart 1): (i) 6AHA and 7AHA, a pair of linear, saturated hydrocarbon chain analogs, (ii) AMCHA, a cyclic aliphatic ligand, and (iii) PAMBA, PAEBA, and BASA, a triad of zwitterions containing aromatic rings. We have also investigated binding of two synthetic peptides: (iv) YLLK, the 119−122 tetrapeptide fragment of the fibrinogen Bβ-chain (Watt *et al.*, 1979), and (v) AFQYHSK, the 44−50 heptapeptide fragment of Glu•Pgn, also known as the Pgn "activation" heptapeptide (Wiman, 1973; Wiman & Wallén, 1975). The activation heptapeptide has been shown to interact with the Pgn/K4 domain (Ramesh *et al.*, 1989) while YLLK was identified as a relatively good ligand in the process of screening for ZxxK tetrapeptide segments within the human fibrinogen sequence, where Z is an aromatic residue and xx are any two bridging amino acids, as potential sites for fibrin−K2 interactions. Perturbations of ^{1}H-NMR signals upon ligand binding were identified and monitored, and values for the K2−ligand equilibrium association constants (K_a) were determined.

An analysis at atomic-level resolution of the binding site interaction with the antifibrinolytic drugs 6AHA and BASA, based on intermolecular ^{1}H−^{1}H NOE constraints, is reported. The ligand titration data, when considered vis-à-vis the binding site structure, lead to an improved appreciation of the molecular factors that contribute to the ligand−K2 interactions.

MATERIALS AND METHODS

The recombinant tPA/K2 domain was generated as published (Cleary *et al.*, 1989). 6AHA, L-Lys, and AMCHA were purchased from Aldrich Chemical Co., while 7AHA

t_m, NOESY mixing time; RMSD, root-mean-square deviation; tPA, tissue-type plasminogen activator; uPA, kidney-type plasminogen activator (urokinase); YLLK, Tyr-Leu-Leu-Lys; 1D, one dimensional; 2D, two dimensional.

Chart 1: Investigated Ligands for Kringle 2

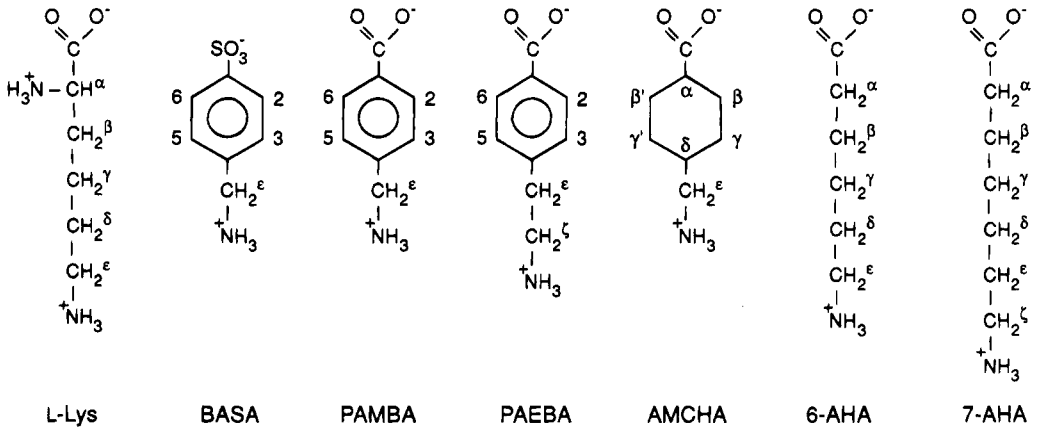

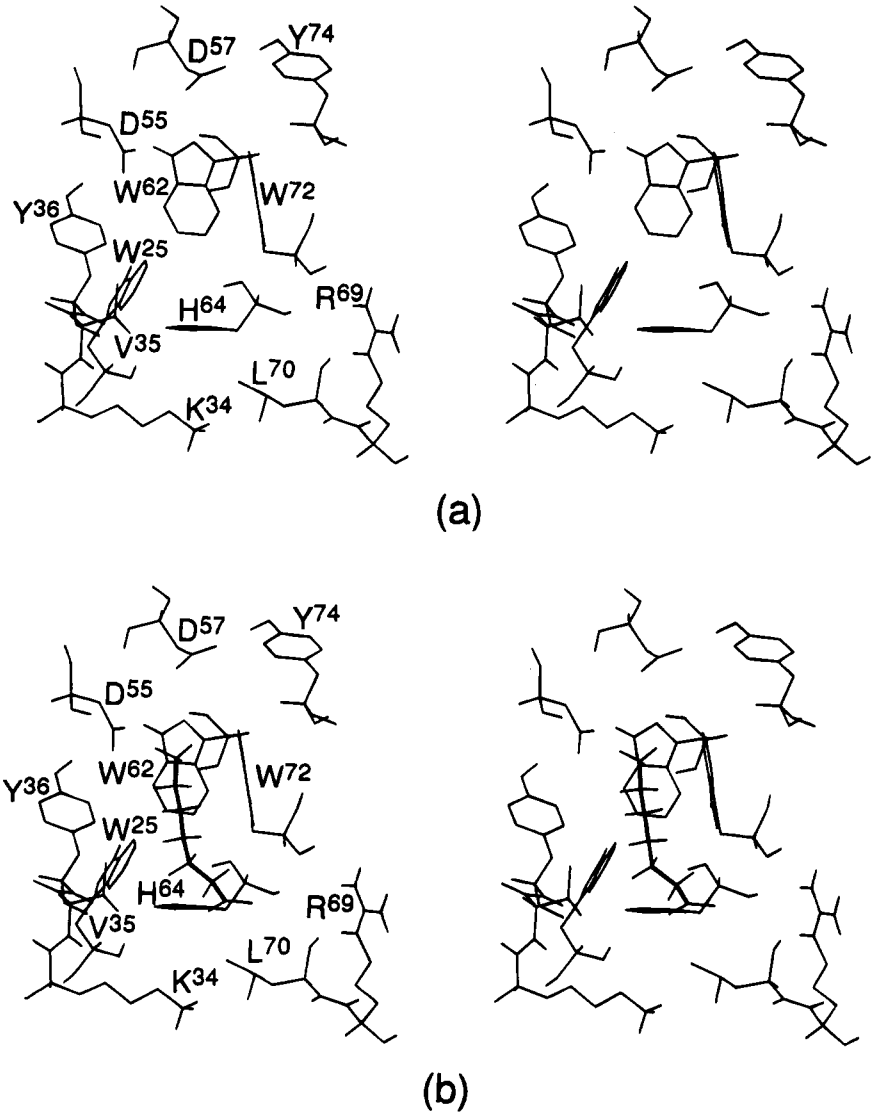

FIGURE 2: Stereoview of the tPA kringle 2 lysine-binding site: (a) ligand-free; (b) occupied by 6AHA. In (b), the ligand is outlined in bold trace. The model was calculated as previously described (Byeon & Llinás, 1991), and the graphics were generated with the program MOL17 (Sneddon, 1990). Leu[46], neighboring the binding site, is omitted in order to simplify the display.

was purchased from Pfaltz & Bauer, Inc. BASA belonged to a batch previously described (Hochschwender *et al.*, 1983). PAMBA and PAEBA were provided by Dr. R. Laursen, Boston University. YLLK and AFQYHSK were synthesized at the peptide synthesis facility of Genentech, Inc.

^{1}H-NMR spectra were recorded on a Bruker AM-500 spectrometer interfaced to an Aspect 3000 computer and an Aspect X32 workstation. 1D NMR spectra in ^2H_2O were acquired with quadrature detection over 32K data points to afford a digital resolution of 0.37 Hz. $^1H^2HO$ signal suppression was achieved by selective presaturation during the 1.5-s equilibrium delay period. Resolution enhancement of 1D spectra was via Gaussian convolution. Chemical shifts are referred to the sodium (trimethylsilyl)[2,2,3,3-^{2}H]propionate resonance using *p*-dioxane as an internal standard (De Marco, 1977).

Phase-sensitive COSY spectra (Wider *et al.*, 1984) in ^2H_2O involved 600−768 t_1 increments (32 scans per t_1 experiment) of 4096 data points. The $^1H^2HO$ signal was suppressed by selective irradiation during the 1.5-s equilibration delay period after each scan. Prior to Fourier transformation, the time domain data in t_2 and t_1 were zero-filled to 8192 and 2048 points to yield digital resolutions of 1.5 and 5.9 Hz in δ_2 and δ_1, respectively, and a sine bell was applied to both dimensions. Phase-sensitive NOESY spectra of the K2 samples in ^1H_2O containing either 6AHA or BASA were recorded as published (Byeon *et al.*, 1991).

Ligand titration experiments were carried out by adding small aliquots of a concentrated (25−50 mM) ligand solution to an ~0.5 mM K2 sample in ^2H_2O, 0.14 M sodium phosphate, pH* 7.2, 25 °C (Byeon *et al.*, 1989). 1D spectra of 128−256 scans each were recorded at each titration point. In the course of each experiment the temperature was increased to 40 °C, and a phase-sensitive COSY spectrum was recorded when the [ligand]/[K2] ratio was ~4. Thereafter, the sample was allowed to equilibrate at 25 °C, and the titration was resumed until saturation was reached, typically at a [ligand]/[K2] ~ 20.

Ligand−kringle interactions are characterized by relatively low affinities (K_a < 1000 mM^{-1}) (Thewes *et al.*, 1990; Rejante *et al.*, 1991b; Kelley *et al.*, 1991; De Serrano *et al.*, 1992b), single site binding, and fast exchange (De Marco *et al.*, 1987). Letting Δ_p stand for the normalized ligand-induced shifts

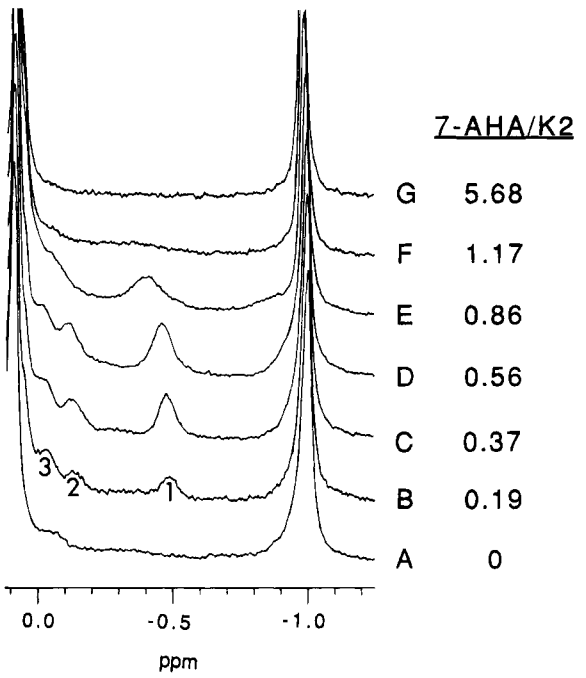

FIGURE 3: ^{1}H-NMR high-field spectra of the kringle 2−7AHA complex. Resonances stemming from bound ligand are labeled 1−3. Large signals at ~−0.97 ppm and ~0.10 ppm arise from K2 Leu[46] and Val[35] methyl protons, respectively.

$$\Delta_p \equiv (\delta_{obs} - \delta_{free})/(\delta_{bound} - \delta_{free}) = [KS]/[K_0] \quad (1)$$

where δ_{obs} is the observed chemical shift of a protein resonance at a certain point in the ligand titration experiment, δ_{free} and δ_{bound} are the limit chemical shifts of the resonance for the ligand-free and ligand-saturated kringle, respectively, [KS] is the concentration of the ligand-bound kringle, and $[K_0]$ is that of the total (free + bound) kringle. The ligand−kringle association constant (K_a) was derived from linearized expressions of eq 1, as reported (De Marco *et al.,* 1987). Depending on the experiment, Δ_p was averaged over four to eight different kringle resonances.

Molecular modeling of the K2−BASA complex was achieved using the program X-PLOR 3.1 (Brünger, 1988) and the experimental NOE constraints. BASA was docked to the K2 binding site, essentially as previously reported for 6AHA (Byeon & Llinás, 1991). The best averaged structure of K2 was used as the initial starting structure [structure $(SA1)_r$] (Byeon & Llinás, 1991). To start, the BASA molecule was manually positioned in proximity to the binding site. One thousand cycles of Powell restrained minimization were run constrained by eight intermolecular NOEs between K2 and the ligand and all of the reported intramolecular NOEs from K2 (Byeon & Llinás, 1991). Since the Lys[34] and Arg[69] side-chain cationic centers are potentially

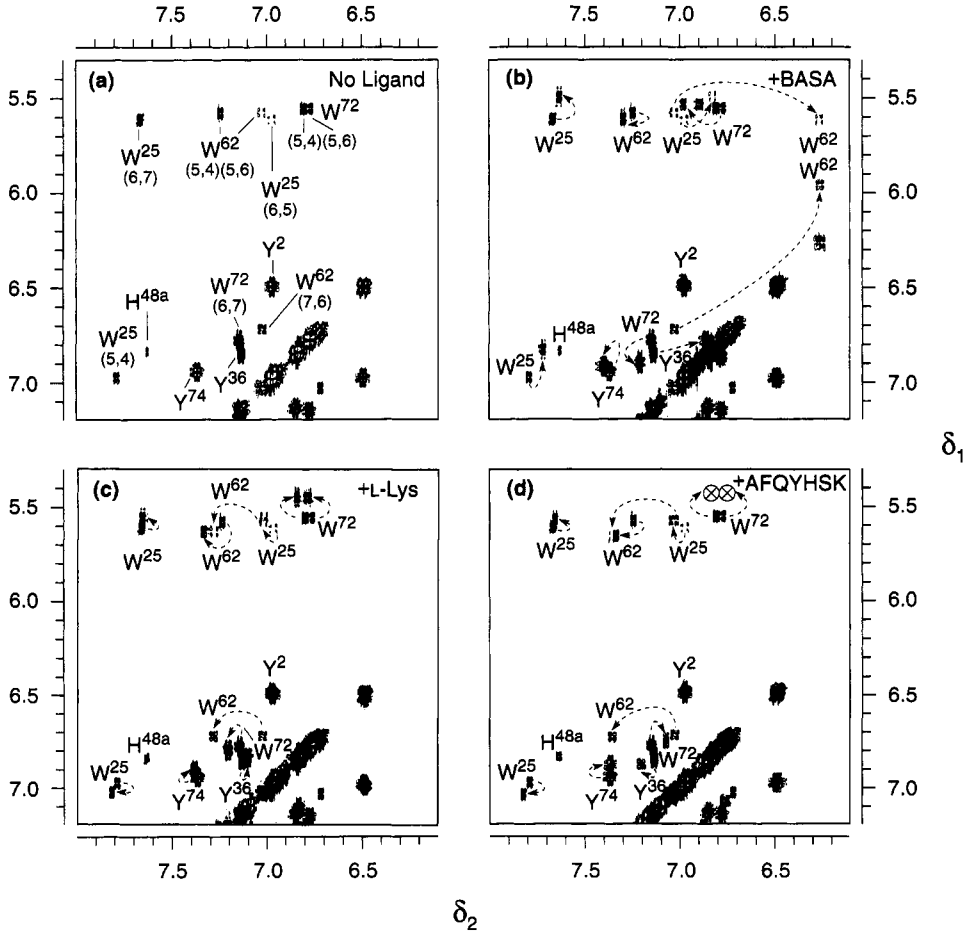

FIGURE 4: Effects of ligands on the kringle 2 aromatic resonances: COSY spectra. Panels: (a) ligand-free K2; (b−d) superpositions on spectrum a of spectra of K2 saturated with BASA (b), L-lysine (c), and AFQYHSK heptapeptide (d). The aromatic cross-peaks from AFQYHSK which appear at 6.82/7.11 ppm (Tyr) and 7.00/7.85 ppm (His) in (d) have been deleted for clarity. Dashed arrows indicate ligand-induced shifts. Broad cross-peaks, apparent at lower contour levels, are denoted by ⊗. Phase-sensitive spectra were recorded on an ~0.5 mM K2 sample in ^2H_2O, 0.1 M sodium phosphate, pH* 7.2, 40 °C; [K2]/[ligand] ~ 1:4.

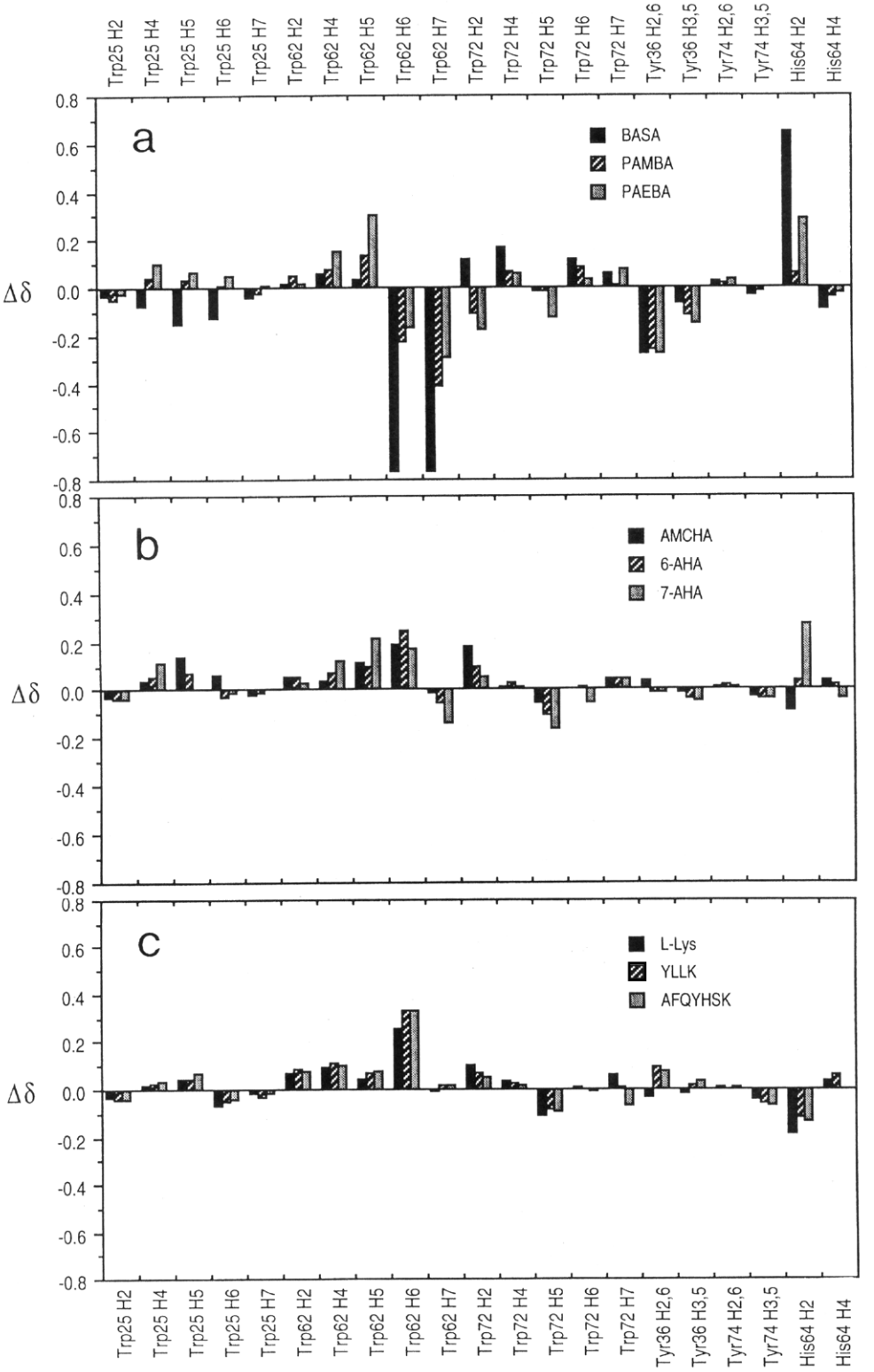

FIGURE 5: Summary of resonance shifts (ppm) caused by the investigated ligands (Chart 1) on kringle 2 aromatic resonances. Bars of positive and negative amplitudes represent ligand-induced low- and high-field shifts, respectively. Panels a, b, and c depict the effects elicited by binding aromatic, aliphatic, and lysyl ligands, respectively. Based on data extracted from COSY spectra as illustrated in Figure 4.

capable of electrostatically interacting with the ligand, two fictitious distance restraints were introduced in order to favor positioning the Lys^{34} and Arg^{69} side-chain cationic groups close to the BASA sulfonate anionic center. Five hundred cycles of Powell restrained minimization were then applied with the two fictitious NOEs turned on, followed by 500 cycles with the fictitious NOEs switched off. In order to account for the nonbonding interactions, Lennard-Jones and Coulombic electrostatic (with distance-dependent dielectric constant) potentials were included.

RESULTS AND DISCUSSION

The molecular model of the tPA/K2 binding site, ligand-free and complexed with 6AHA, is shown in Figure 2. Below, we present ^{1}H-NMR evidence supporting the proposed structure.

Aromatic Character of the Binding Site. Figure 3 shows the ^{1}H-NMR $-1.25 < \delta < 0.12$ ppm spectral region of the tPA/K2 in the absence of ligand (A) and in the presence of increasing levels of added 7AHA (B−G). Three signals (labeled 1−3) emerge from the background in response to a minimal addition of ligand (B). These grow in intensity as more ligand is present (C, D) and eventually broaden while shifting to low field (E−G) to appear, at large ligand excess, close to the unbound 7AHA spectral positions ($2.3 > \delta > 1.5$ ppm). The shifts and broadening of ligand resonances hinge on the residence time of the ligand at the binding site, therefore on the dissociation rate constant k_{off}. Thus, depending on K_a ($=k_{on}/k_{off}$), i.e., on the ligand on/off exchange kinetics, shifted ligand signals are variously detected (Llinás *et al.*, 1985; De Marco *et al.*, 1987). At substoichiometric ligand levels, conditions under which the ligand is mostly bound, the 7AHA resonances result drastically shifted, reflecting local diamagnetic shieldings arising from the protein environment at the binding site. In the case of Pgn/K4, these have been assigned to anisotropic ring-current effects caused by aromatic side chains which contact, via hydrophobic interactions, bound ligand methylene groups (Ramesh *et al.*, 1987; Petros *et al.*, 1989). Therefore, the experiment illustrated in Figure 3 affords evidence pointing to close ligand−aromatic ring contacts in the tPA/K2 as well.

Ligand-Binding Effects on K2 Aromatic Side Chains. An effect that complements the one described above is the perturbation of kringle aromatic resonances resulting from ligand binding. COSY spectra that illustrate these effects for the ligands BASA, L-Lys, and AFQYHSK are shown in Figure 4 b−d. Figure 5 summarizes the shifts induced by the investigated ligands. It is apparent that essentially the same set of aromatic residues, namely Trp^{25}, Tyr^{36}, Trp^{62}, His^{64}, Trp^{72}, and Tyr^{74}, are consistently affected by ligand binding. Except for Tyr^{74}, these aromatic side chains exhibit shifts which are sensitive to ligand structure. The response of Tyr^{74}, in contrast, is minor and rather uniform, which suggests that it senses ligand binding indirectly, through interactions with neighboring groups that do contact the ligand. Consistent with the model (Figure 2), substituting Tyr^{74} for other residues is of little consequence for the ligand-binding properties of K2 (De Serrano & Castellino, 1994b). We note that the effects illustrated in Figures 4 and 5 are quite specific when compared to the minute perturbations observed on the remainder of the aromatic side chains: Tyr^2, His^{48a}, Phe^3, Tyr^9, His^{13}, and Tyr^{50}. Predictably, it is the aromatic ligands which, via their own anisotropic shielding effects, most markedly perturb the K2 spectrum (Figure 5a).

Interestingly, the His^{64} imidazole H2 resonance is uniformly shifted by ~−0.15 ppm by L-Lys and by the two peptides (Figure 5c), which contrasts the opposite (low-field) shifts elicited by noncyclic analogs which lack an α-substituent group (Figure 5b). It is noticeable that, overall, the perturbations caused by the two peptides on the K2 aromatic spectrum mimic closely those elicited by the free L-Lys ligand (Figures 4c,d and 5c), affording strong evidence that the two peptides bind K2 through the C-terminal Lys residue, which affords the canonical zwitterionic kringle anchoring group.

Aliphatic Residues at the Binding Site. Spectra in Figure 6 illustrate shifts of K2 aliphatic resonances resulting from binding ligands. Aromatic ligands variously perturb the Val^{35} H$^{\beta}$, the Asp^{55} H$^{\beta,\beta'}$, and, to a lesser extent, the Leu^{31}, Val^{35}, and Leu^{46} methyl signals (Figures 6b and 7a). Similar perturbations are caused by L-Lys, YLLK, and AFQYHSK (Figures 6c,d and 7c). However, while the Asp^{55} H$^{\beta'}$ resonance results significantly shifted by the two peptides ($\Delta\delta \sim -0.1$ ppm), it is essentially unaffected by L-Lys. It is also noteworthy that L-Lys and the two peptides perturb the Val^{35} side-chain resonances much more extensively than 6AHA does (Figure 7b,c), confirming that the ligand α-amino group positions itself proximal to the Val^{35} side chain (Figure 2b).

The perturbations on the K2 aliphatic spectrum elicited by 6AHA, 7AHA, and AMCHA are analogous to those induced by L-Lys (Figures 6c and 7b,c). It is curious that the Asp^{55} H$^{\beta,\beta'}$ resonances are shifted to low fields ($\Delta\delta \sim 0.09$ ppm) by the cyclic aliphatic ligand AMCHA but, less markedly, to high fields by 6AHA and 7AHA. This is likely to reflect the lesser flexibility of the AMCHA ring when the molecule accommodates itself for ionic pairing with the Asp^{55} $^{\gamma}$COO$^-$ group (see below).

Kringle 2−Ligand Contact Points. Figure 8 shows the aromatic NOESY spectrum of K2 saturated with BASA. Strong and weak intermolecular NOEs are observed between the K2 Tyr^{36} aromatic and the BASA ring H2,6 *(ortho)* and H3,5 *(meta)* protons (Chart 1), respectively. It is noteworthy that the intensities of the cross-peaks correlate well with the amplitudes of BASA-induced shifts elicited on the Tyr^{36} aromatic signals (Figures 4b and 5a). The BASA H2,6 protons also exhibit intermolecular NOEs with the Trp^{62} indole H6 (Figure 8). This concurs with the ligand-induced shifts as well since a marked perturbation is observed for the Trp^{62} H6 aromatic resonance upon BASA binding (Figure 4b). An NOE between the BASA H2,6 and the Trp^{72} indole H2 protons is also apparent (Figure 8) which, as is the case for the other contacts, correlates well with the Trp^{72} H2 resonance being most sensitive to ligand presence (Figure 5a). Finally, a close interaction between the His^{64} imidazole H2 and the BASA aromatic ring protons was identified from magnetization transfer experiments at 300 MHz in the course of which 500-ms preirradiation was applied at the His^{64} H2 transition frequency and a strong NOE resulted on the BASA H2,6 signal (not shown; experimental conditions: ^2H_2O solution, 0.14 M sodium phosphate, pH* 7.2, 40 °C). This, as already noticed for the other residues, is consistent with the His^{64} imidazole signals undergoing sizable shifts upon BASA binding (Figure 5a).

In the course of BASA titration experiments, we have observed that, under conditions of ligand excess relative to K2, BASA signals arising from the methylene H$^{\epsilon,\epsilon'}$ and aromatic H3,5 resonances proximal to the amino end of the molecule appear severely broadened relative to those from the aromatic H2,6 atoms (not shown). A similar pattern of broadening of BASA resonances has previously been reported for the ligand interacting with the Pgn/K4 (Llinás *et al.*, 1985). Since the ligand exchanges between free in solution and K2-bound states, the differences in line widths suggest that the amino end group of the molecule senses the binding site environment in a more intimate fashion than does the sulfonate end, the latter being relatively more mobile and solvent-exposed.

Expansions of the NOESY aromatic spectral region of the K2/6AHA complex are shown in Figure 9. As observed for the BASA complex, the ligand interacts with the Tyr^{36}, Trp^{62}, His^{64}, and Trp^{72} aromatic groups. On the other hand, (i)

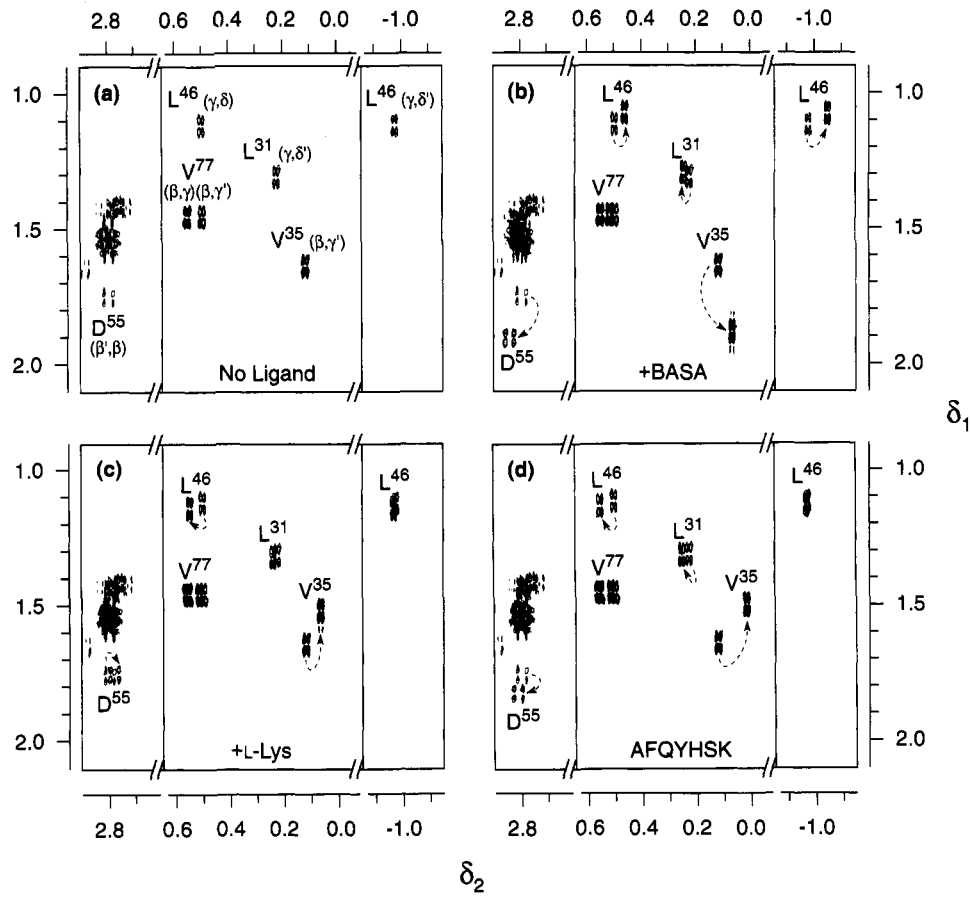

FIGURE 6: Effects of ligands on the kringle 2 aliphatic resonances: COSY spectra. Panels: (a) ligand-free K2; (b–d) superpositions on spectrum a of spectra of K2 saturated with BASA (b), L-lysine (c), and AFQYHSK heptapeptide (d). Dashed arrows indicate ligand-induced shifts. Experimental conditions are the same as for Figure 4.

while the Trp^{72} indole NH1 shows NOEs with 6AHA protons, we do not detect such a contact with BASA; (ii) the Tyr^{36} ring exhibits NOEs with the BASA H3,5 (positionally analogous to the $H^{\gamma,\gamma'}$ in 6AHA) as well as the H2,6 (positionally analogous to the $H^{\beta,\beta'}$ in 6AHA) protons while, in the case of 6AHA, only interproton interactions between the Tyr^{36} aromatic ring and ligand $H^{\alpha,\alpha'}$ and $H^{\beta,\beta'}$ sites are detected. Furthermore, we notice that 6AHA interacts with the Trp^{62} indole H5 and H6 while in the case of Trp^{72} the ligand mainly contacts its H1 and H2 sites (Figure 9). It is also apparent that, as discussed above for BASA, the His^{64} imidazole H2 interacts closely with 6AHA (Figure 9). Again, as for the BASA complex, the relative intensities of the intermolecular NOEs connecting the Trp^{62}, Trp^{72}, and His^{64} side chains to 6AHA parallel the magnitudes of the shifts caused by the ligand on the corresponding aromatic resonances (Figure 5b).

Ligand Docking at the Binding Site. According to the model (Figure 2b), the Tyr^{36}, Trp^{62}, His^{64}, and Trp^{72} aromatic groups exhibit direct interactions with the ligand. The Trp^{62} and His^{64} side-chain rings are located at structurally constrained loci, and their accessibility to solvent appears reduced upon ligand binding. In contrast, the Trp^{72} and the Tyr^{36} rings lie on the surface, positioning themselves right and left of the Trp^{62} and His^{64} rings, respectively. Hence, exposure of the Trp^{72} and Tyr^{36} side chains results relatively less affected by ligand binding. We note that the Trp^{62} and Trp^{72} indole rings contact each other by conforming a V-shaped groove. This improves a preliminary model in which the two indole rings were placed parallel relative to each other (Tulinsky *et al.*, 1988) and is consistent with the more recent structures of the complexed Pgn/K4, derived via X-ray crystallography (Wu *et al.*, 1991) and NMR spectroscopy (Cox *et al.*, 1994). The crucial role of Trp^{72} in ligand binding in the Pgn/K4 had been established by chemical modification and NMR studies (Hochschwender & Laursen, 1981; Llinás *et al.*, 1983) and in the tPA/K2 predicted by homology/modeling (Tulinsky *et al.*, 1988) and confirmed by NMR (Byeon *et al.*, 1989) and site-directed mutagenesis (de Vos *et al.*, 1992; De Serrano & Castellino, 1992a) studies. The structure (Figure 2) further shows that the Trp^{62} indole NH1 hydrogen is placed between the Asp^{55} and Asp^{57} carboxylate groups, which is consistent with the observed pH titratability (with inflections at pH ~5.1 and ~4.1) of the NH1 resonance (Byeon *et al.*, 1989).

The ligand distal amino group positions itself proximal to the Asp^{55} carboxylate group (Figure 2b), in harmony with the Asp^{55} $H^{\beta,\beta'}$ resonances being significantly perturbed by 6AHA (Figure 7b). The Asp^{57} carboxylate group also appears in the proximity, the model suggesting a relatively larger distance to the ligand ϵ-amino group (~3.7 Å) so that their mutual electrostatic interaction is likely to be somewhat weaker than for Asp^{55} (~2 Å). However, as evidenced by chemical modification (Trexler *et al.*, 1982) and mutagenesis experiments (De Serrano & Castellino, 1993), there can be only little doubt as to the relevance of Asp^{57} in ω-amino acid ligand binding to kringles.

In contrast to what is the case for the ligand amino group, the ligand carboxylate group exhibits relatively less defined interactions with the cationic side-chain groups of Lys^{34} and

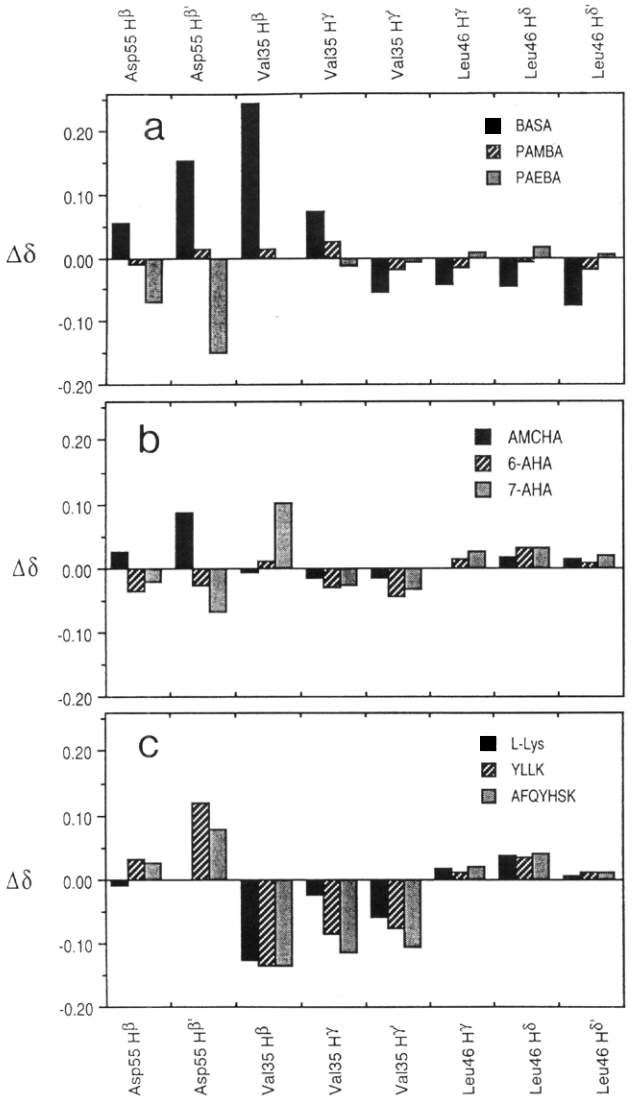

FIGURE 7: Summary of resonance shifts (ppm) caused by the investigated ligands (Chart 1) on kringle 2 aliphatic resonances. Bars of positive and negative amplitudes represent ligand-induced low- and high-field shifts, respectively. Panels a, b, and c depict the effects elicited by binding aromatic, aliphatic, and lysyl ligands, respectively. Based on data extracted from COSY spectra as illustrated in Figure 6.

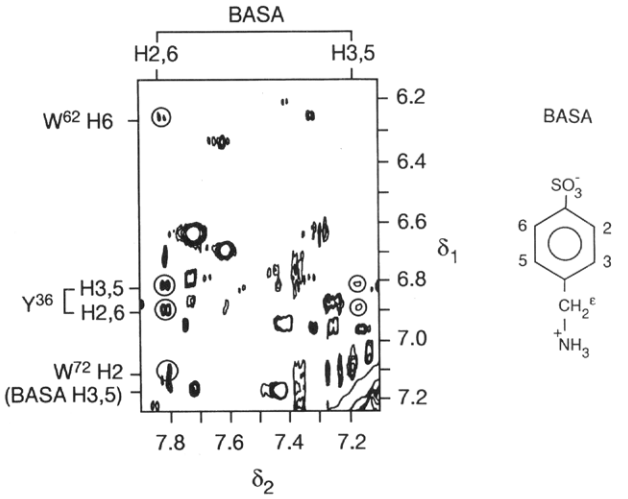

FIGURE 8: ^{1}H-NMR NOESY spectrum of kringle 2 in the presence of BASA: aromatic region. Intermolecular connectivities are circled. A cross-peak linking the Trp^{62} indole H5 to the BASA ring H2,6 sites appears at 5.57/7.82 ppm (not shown). Spectrum recorded on an ~4 mM K2 sample dissolved in ^2H_2O, 0.14 M ammonium sulfate, pH 4.9, 63 °C; [K2]/[BASA] ~ 1:6.

Table 1: Kringle 2−Ligand Association Constants

ligand	K_a (mM^{-1}) NMR[a]	K_a (mM^{-1}) calorimetry[b]
L-Lys	17.9 ± 0.5	15.5
6AHA	21.7 ± 0.3	19.3
7AHA	149.3 ± 4.7	189.0
YLLK	37.3 ± 2.0	
AFQYHSK	37.6 ± 1.5	
AMCHA	69.4 ± 3.7	51.2
PAMBA	31.3 ± 0.8	
PAEBA	11.7 ± 0.3	
BASA	232.6 ± 16.3	

[a] K_a values were estimated from 1D ^{1}H-NMR ligand titration experiments. Experimental conditions: ~0.5 mM kringle 2 dissolved in ^2H_2O, 0.1 M sodium phosphate, pH* 7.2, 25.0 °C. [b] K_a values determined by microcalorimetry (Kelley *et al.*, 1991). Experimental conditions: K2 dissolved in ^2H_2O, 0.15 M sodium acetate, 0.05 M Tris−acetate, pH 8, 25.4 °C. The standard error for the measured values is <20%.

Arg^{69}. In analogy to what is the case for BASA, in the presence of K2 the 6AHA distal δ- and ϵ-methylene resonances appear markedly broadened, while the α- and β-protons at the carboxylate end yield relatively narrow signals (not shown). By reference to the binding site structure (Figure 2), this observation reinforces a model whereby the amino end of 6AHA interacts with the K2 binding site more intimately than does the carboxylate end of the molecule. Hence, it is suggested that the ligand ϵ-amino group fulfills a more critical role for binding to K2 than its corresponding carboxylate group. This contention is consistent with ligand-binding data for Pgn/K4 showing that ligand analogs lacking the distal cationic center interact negligibly while those missing the carboxylate group do bind, albeit with significantly reduced affinities (Rejante *et al.*, 1991b).

The Tyr^{74} and Trp^{25} aromatic rings neighbor the binding site but do not directly contact the ligand (Figure 2b). This concurs with the observation of only minor spectral perturbations caused by the ligand on these residues and the absence of detectable intermolecular NOEs (Figure 9). Indeed, K2 variants generated via conservative site-specific mutagensis of the two residues are mostly marginally affected in their ligand-binding properties (De Serrano & Castellino, 1994a,b). The Val^{35} side chain is located at the binding site and establishes good contact with the ligand β- and γ-methylene groups (Figure 2b). The ligand-induced shifts exhibited by the Val^{35} resonances (Figure 7) are, therefore, likely to result from such an interaction.

Ligand Affinities. Ligand titration curves were obtained by monitoring induced shifts of selected K2 resonances at various ligand concentrations. Figure 10 illustrates the results of such experiments for the aromatic ligands. From the binding profiles, ligand−kringle association constant (K_a) values were derived (see Materials and Methods). Table 1 lists the NMR K_a values, together with those estimated from microcalorimetry experiments (Kelley *et al.*, 1991).

YLLK and AFQYHSK show essentially the same affinity (K_a ~ 37 mM^{-1}) toward K2, their association constants being ~2-fold larger than those measured for L-lysine (K_a ~ 17.9 mM^{-1}). As indicated by the ligand-induced spectral per-

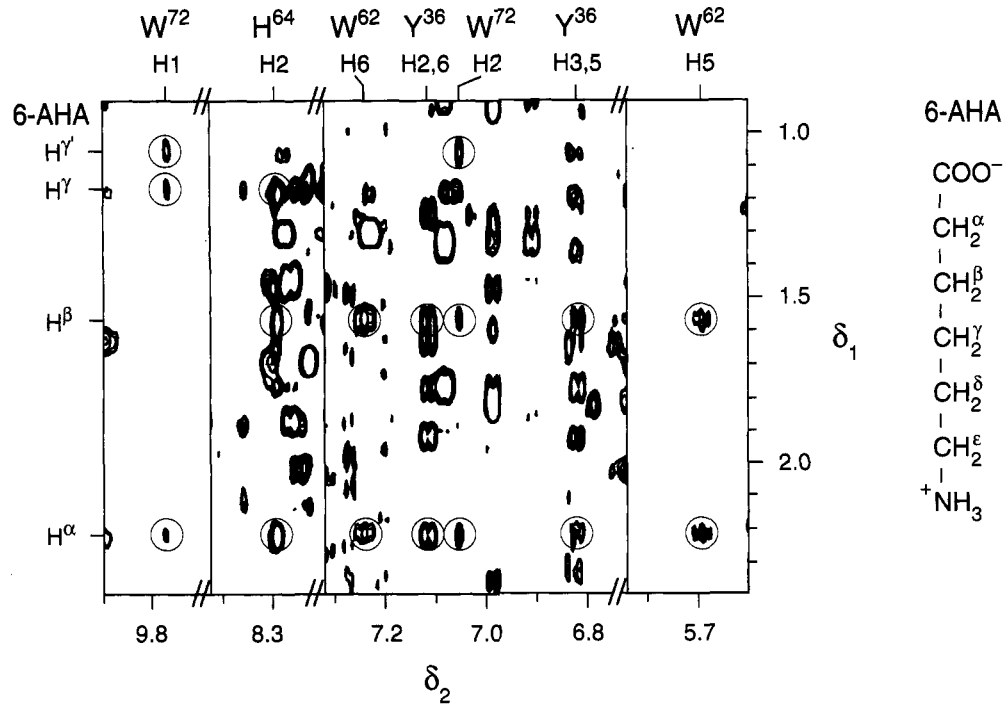

FIGURE 9: ^{1}H-NMR NOESY spectrum of kringle 2 in the presence of 6AHA: contacts between protein and ligand. Intermolecular cross-peaks are circled. Spectrum recorded on an ~ 2 mM K2 sample dissolved in salt-free ^1H_2O, pH 4.9, 53 °C; [K2]/[6AHA] ~ 1:6.

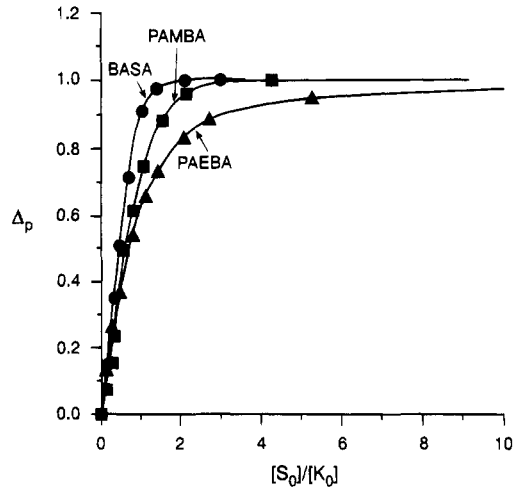

FIGURE 10: Interaction of tPA kringle 2 with aromatic ligands: ^{1}H-NMR ligand titration profiles. Δ_p, the fraction of ligand-bound kringle, is plotted against $[S_0]/[K_0]$, the ratio of total ligand concentration to total kringle concentration: BASA (●); PAMBA (■); PAEBA (▲).

turbations (Figures 4−7), most likely it is the C-terminal Lys residue that anchors the peptides at the binding site. Moreover, the higher affinity exhibited by these peptides relative to the free amino acid, L-lysine, indicates that the attached polypeptide segments contribute positively to their binding to K2. An increased affinity relative to L-lysine has also been observed for N^{α}-acetyl-L-lysine (K_a ~ 57 mM^{-1}) (Kelley *et al.*, 1991), suggesting that blockage of the positively charged α-amino group favors binding and is consistent with the slightly stronger binding of 6AHA (K_a ~ 21.7 mM^{-1}) relative to L-lysine. A similar trend was observed in the case of the Pgn/K4 (Rejante *et al.*, 1991b) and was interpreted as reflecting a possible electrostatic interference of the ligand cationic α-amino group with the ligand anion interacting with the positive electrostatic potential originating from the Lys^{36} and/or Arg^{71} polar groups. Probably not fortuitously, the Pgn/K5, which lacks such cationic centers (instead, it carries Phe^{36} and Leu^{71}), exhibits a marked preference for hexylamine relative to L-lysine (Thewes *et al.*, 1990). However, a purely electrostatic interaction is unlikely to be the sole cause for the higher stability of the YLLK and AQYHSK peptides since other Lys C-terminal fibrinopeptides that were investigated showed a lesser tendency for complex formation with the tPA/K2 (M. G. Mulkerrin, unpublished), which may be of significance for identifying possible sites of interaction between fibrin and tPA.

While the 6AHA aliphatic chain may be slightly too short to bridge close contacts with both the Lys^{34} and Arg^{69} side-chain polar groups, the mutagenesis experiments of De Serrano and Castellino (1992b) reveal that binding of ω-amino acid ligands is drastically lowered by mutating Lys^{34} to a variety of other amino acids and measurably weakened by an Arg^{69} → Ala substitution, suggesting that both cationic centers contribute to the positive electrostatic field that interacts with the anionic end of the ligand molecule. 7AHA, a one-methylene unit (1.2 Å) longer linear chain analog (Chart 1), exhibits an ~7-fold higher affinity (K_a ~ 149 mM^{-1}) relative to the linear ligand analogs 6AHA and L-Lys. The enhanced affinity of 7AHA may be rationalized from the binding site structure (Figure 2) which suggests that, while docked at the binding site, the 7AHA carboxylate group can more readily access the Arg^{69} cationic center of K2. We also note that the carboxylate group of 6AHA places itself proximal to the Leu^{70} methyl groups, hinting at an energetically wasteful hydrophobic−polar contact. In the case of 7AHA, the ligand α-methylene group can position itself relatively closer to the Leu^{70} methyl groups, thus favoring lipophilic interactions with the kringle.

AMCHA shows ~3.6-fold higher affinity toward K2 (K_a ~ 69 mM^{-1}) than the linear chain analogs 6AHA and L-Lys (Table 1). This may stem from a more extensive surface interaction between the cyclohexyl ring and the aromatic side

chains that line the binding site. It also implies that the lipophilic binding pocket is ample enough to accommodate the cyclic ligand hydrocarbon ring. A relatively high affinity toward AMCHA has previously been observed for Pgn/K1 (K_a > 300 mM^{-1}) (Menhart *et al.*, 1991; Rejante, 1992), K4 (K_a ~ 159 mM^{-1}) (Markus *et al.*, 1981; De Marco *et al.*, 1987; Rejante *et al.*, 1991b), and K5 (K_a ~ 45 mM^{-1}) (Menhart *et al.*, 1993).

By comparison to 6AHA or L-Lys, PAMBA shows ~1.5 times higher affinity (K_a ~ 31 mM^{-1}), which indicates that ligand aromaticity contributes positively to the binding. However, PAMBA turns out to be a weaker ligand than AMCHA, suggesting a potential stabilization conferred by the chair ↔ boat conformational adaptability of the AMCHA cyclohexyl ring. The lower affinity of PAMBA toward the tPA/K2 is not surprising in view of the relative weak binding of PAMBA to Pgn/K1 (K_a ~ 13 mM^{-1}) (Rejante, 1992) and K4 (K_a ~ 4.8 mM^{-1}) (Rejante *et al.*, 1991b).

In contrast to what is observed on going from 6AHA to 7AHA, lengthening the PAMBA molecule by one methylene unit to generate PAEBA lowers its affinity to K2 to K_a ~ 12 mM^{-1}. In terms of the binding site structure (Figure 2), the aminoethyl group in PAEBA, displaced toward Asp^{55} + Asp^{57}, is bound to cause the ligand ring to displace itself away from its optimal position (relative to PAMBA) at the binding site by decreasing its interaction with the lipophilic aromatic surface. This would bring the PAEBA phenyl group to juxtapose against the protruding Val^{35} and Leu^{70} methyl groups, which could affect binding because of steric hindrance.

It is noteworthy that, relative to PAMBA, its closest aromatic analog, BASA, exhibits ~ 7.5-fold higher affinity for K2 (K_a ~ 232 mM^{-1}) (Table 1). This indicates that the significantly more polar sulfonate group favors binding to K2. An increased affinity toward BASA was also observed in the case of the Pgn/K1 (K_a ~ 82 mM^{-1}) and K4 domains (K_a ~ 74 mM^{-1}) (De Marco *et al.*, 1987; Rejante *et al.*, 1991b; Rejante, 1992) and is consistent with the known preference of protein Arg and Lys cationic centers to complex sulfate groups (Kanyo & Christianson, 1991). Indeed, in the Pgn/K4 crystallographic structure, a sulfate anion is found complexed to Lys^{36} and Arg^{71} (Mulichak *et al.*, 1991). Furthermore, it is apparent that, among the tested ligands, BASA shifts the K2 spectrum the most (Figures 4−7). The exaggerated perturbation, an amplified anisotropic ring-current shielding effect induced by the ligand on protein resonances, reveals intimate intermolecular BASA−side-chain interactions at the binding site as indicated by the NOESY experiment (Figure 8).

A molecular model of the K2−BASA complex (Figure 11) was generated from the experimental intermolecular NOE constraints as described under Materials and Methods. The backbone structure of the K2−BASA complex results to be not much different from that of the K2−6AHA complex (RMSD of 0.66 Å for the backbone and 0.93 Å for all atoms). Expectedly, the occupied binding pocket of K2−BASA is similar to that of the K2−6AHA complex (Figure 2), showing the BASA amino group to be closer (~2.6 Å) to the γ-carboxylate group of Asp^{55} (ion pair interaction) than to that of Asp^{57} (~3.8 Å). As to the cationic groups, the Lys^{34} $^{\epsilon}NH_3^+$ positions itself more proximal to the BASA sulfonate group than does the Arg^{69} guanidino group (~3.8 *vs* ~4.8 Å). The model also reveals close stacking between

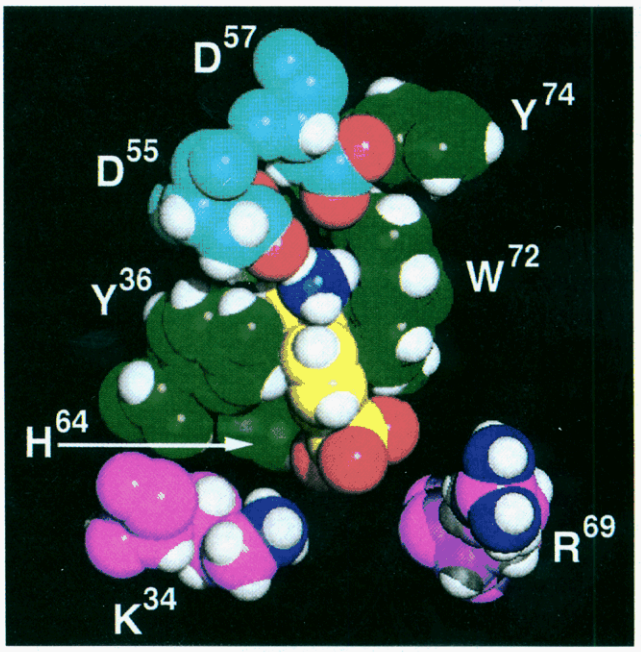

FIGURE 11: NMR structure of the kringle 2−BASA complex: view of the binding site. The space-filling model was generated with the graphics program Quanta (Molecular Simulations Inc., Waltham, MA). The ligand is shown in yellow. K2 side chains are shown in purple for basic residues (K^{34}, R^{69}), in light blue for acidic residues (D^{55}, D^{57}), and in green for aromatic residues (Y^{36}, H^{64}, W^{72}, Y^{74}). Polar group N and O atoms are shown in blue and red, respectively.

BASA and the kringle Tyr^{36} and Trp^{72} aromatic rings (Figure 11). The average ring-to-ring intercarbon distances between BASA and Tyr^{36}, His^{64}, Trp^{62}, and Trp^{72} are about 4.6, 5.9, 5.6, and 4.8 Å, respectively. Such a close hydrophobic packing should afford a major stabilization to the complex, further contributing to the significantly higher affinity of K2 for BASA (K_a ~ 232 mM^{-1}).

CONCLUSIONS

We have investigated interactions between the tPA/K2 domain and nine structurally different ω-aminocarboxylic acid ligands, including two peptides with a C-terminal Lys residue. Although the magnitude of the induced ^{1}H-NMR shifts varies, it is apparent that basically the same set of K2 resonances are affected by the various ligands. These include the Tyr^{36}, Trp^{62}, His^{64}, Trp^{72}, and Tyr^{74} aromatic signals (Figures 4 and 5). Once conservative substitutions at sites 36, 64, and 72 are taken into account, it is concluded that the binding site of tPA/K2 is structured by an array of aromatic residues, fundamentally analogous to that described for the Pgn/K1, K4, and K5 binding sites (Motta *et al.*, 1987; Rejante, 1992; Ramesh *et al.*, 1987; Tulinsky *et al.*, 1988; Thewes *et al.*, 1990). A close positioning of ligand molecules against aromatic rings is indicated by the drastic diamagnetic shifts experienced by the 7AHA methylene protons upon binding to K2 (Figure 3).

Ligand binding also induces a number of shifts on aliphatic side-chain resonances, most prominent for the Val^{35} and Leu^{46} methyl and Val^{35} CH^{β} and Asp^{55} $CH^{\beta,\beta'}$ signals (Figures 6 and 7), consistent with location of these residues at or neighboring the binding site (Figure 2). In the case of the Pgn/K1, K4, and K5, the Asp^{55} γ-carboxylate group has long been a prime candidate for interactions with the ligand ϵ-amino group (Lerch & Rickli, 1980; Thewes *et al.*, 1987),

a contention that is supported by the crystallographic structure of the K4-6AHA complex (Wu *et al.*, 1991). As to Asp[57], its resonances could not be monitored because of difficulty in identifying the broad, quasi-degenerate, $CH^{\beta,\beta'}$ multiplets (Byeon *et al.*, 1991). However, integrity of the Asp[57] residue has been shown to be crucial for lysine binding to Pgn/K4 (Trexler *et al.*, 1982; Nielsen *et al.*, 1993),, and both the NMR (Byeon & Llinás, 1991) and crystallographic (de Vos *et al.*, 1992) structures of the tPA/K2 show Asp[57] to be optimally positioned for interaction with the ligand. Consistently, the crystallographic structure of the K4-6AHA complex indicates the Asp[57] anionic center ion pairs with the ligand cationic group (Wu *et al.*, 1991).

Main features of the ligand-binding interaction can be rationalized from the K2 structure. The binding site (Figure 2) exhibits three characteristic regions: (i) an anionic center composed of the Asp[55] and Asp[57] carboxylate groups; (ii) a lipophilic, mostly aromatic, binding pocket in which the Trp[62] and His[64] side chains line an exposed surface confined laterally by the Tyr[36] and Trp[72] rings, with Val[35] and Leu[70] methyl groups contributing extra hydrophobic character to the site; (iii) a cationic center configured by Lys[34] reinforced by the Arg[69] side chain. The structure is thus consistent with the ligand $H^{\epsilon,\epsilon'}$ and $H^{\delta,\delta'}$ resonances undergoing severe broadening upon binding to K2 while the corresponding $H^{\alpha,\alpha'}$ and $H^{\beta,\beta'}$ signals are barely affected. Indeed, the model (Figure 2b) shows the ligand's distal cationic amino group positioned at the deeper, capped end of the binding pocket while its carboxylate group, lying at the opposite region of the binding site, interacts rather loosely with a more shallow and unhindered area. Consistent with this picture, the electropositive monopoles provided by Lys[34] and Arg[69] exhibit poorly defined locations, a result of their attachment to longer, structurally flexible and solvent-exposed, side chains. This contrasts the situation at the Asp[55] + Asp[57] locus. The fact that AMCHA, despite representing the highest affinity ligand known for the Pgn/K1 ($K_a \sim 1000$ mM^{-1}) (Menhart *et al.*, 1991; Rejante, 1992) and K4 ($K_a \sim 159$ mM^{-1}) (Marcus *et al.*, 1981; De Marco *et al.*, 1987), exhibits a relatively lower affinity for the tPA/K2 ($K_a \sim 69$ mM^{-1}) (Table 1) might be related to the fact that its dipole length, ~6.7 Å, is considerably less than 8.5 Å, the optimum suggested by 7AHA. Overall, it is satisfying that the ligand-induced spectroscopic perturbations (Figures 4−7), Overhauser connectivities (Figures 8 and 9), and the computed structures (Figures 2 and 11) harmonize remarkably well while concurring with studies of site-specific mutants (Kelley *et al.*, 1991; de Vos *et al.*, 1992; De Serrano & Castellino, 1992a,b, 1993, 1994a,b).

From a functional standpoint, it is noteworthy that the two peptides investigated, YLLK, identified after screening a number of potential Lys C-terminal fibrinopeptides, and the Pgn "activation" heptapeptide AFQYHSK, bind to K2 with an affinity ($K_a \sim 37$ mM^{-1}) which is about twice as large as that exhibitted by L-Lys itself ($K_a \sim 18$ mM^{-1}). The two peptides contain a Tyr residue at position −4 relative to the C-terminus which suggests a possible stabilizing role for the aromatic ring while binding to the kringle (Rajan, 1987). AFQYHSK is known to bind to the Pgn/K4, albeit with lower affinity, $K_a \sim 7$ mM^{-1} (Ramesh *et al.*, 1989).

Chart 2 lists amino acid residues that contribute to the binding site anionic center and aromatic pocket in human tPA, uPA and Pgn, and bovine Ptb kringles. The chart

Chart 2: Homology at Sites 55, 57, 62, 64, and 72 in Kringle Sequences

	55	57	62	64	72
tPA/K2	Asp	Asp	Trp	His	Trp
Pgn/K1	Asp	Asp	Trp	Tyr	Tyr
Pgn/K4	Asp	Asp	Trp	Phe	Trp
Pgn/K5	Asp	Asp	Trp	Tyr	Tyr
Pgn/K2	Asp	Glu	Trp	Phe	Trp
Pgn/K3	Asp	Lys	Trp	His	Trp
uPA/K	Asp	Arg	Trp	Tyr	Val
Ptb/K1	Asp	Ser	Trp	Tyr	Arg
Ptb/K2	Asp	Asp	Trp	Tyr	Asp
tPA/K1	Asp	Asp	Trp	Tyr	Ser

excludes basic residues providing the cationic centers as they tend to appear at variable positions in the sequence: e.g., Lys[34] and/or Arg[69] in tPA/K2 (Byeon & Llinás, 1991; De Serrano & Castellino 1992b), Lys[34] and/or Arg[71] in Pgn/K1 (Váli & Patthy, 1984; Motta *et al.*, 1987; Rejante & Llinás, 1994), and Lys[36] and/or Arg[71] in Pgn/K4 (Trexler *et al.*, 1982; Ramesh *et al.*, 1987; Mulichak *et al.*, 1991; Nielsen *et al.*, 1993; Cox *et al.*, 1994). It is apparent that the tPA/K2 and the Pgn/K1, K2, K4, and K5—all ω-amino acid binding kringles—satisfy the polar anionic and aromatic structural/functional requirements for configuring a *bona fide* binding site. In contrast, Ptb/K1 and the uPA/K, which fail to bind lysine, fill position 72 with aliphatic residues and site 57 with nonacidic residues. Similarly, the Ptb/K2, which is not known to bind lysine, misses an aromatic residue at site 72, a feature known to be crucial in the case of Pgn kringles (Hochschwender & Lausen, 1981; Llinás *et al.*, 1983; Thewes *et al.*, 1990) and the tPA/K2 (Byeon & Llinás, 1991; de Vos *et al.*, 1992; De Serrano & Castellino, 1992a).

Pgn/K5 lacks basic residues at sites 34 and 71 although it contains, as is the case for the tPA/K2, a neighboring Arg residue at site 69. Not surprisingly, it binds 6AHA ($K_a \sim 11$ mM^{-1}; Thewes *et al.*, 1990) but with about half the affinity shown by the Pgn/K4 ($K_a \sim 21$ mM^{-1}; De Marco *et al.*, 1987) or the tPA/K2 ($K_a \sim 22$ mM^{-1}; Table 1). Similarly, the Pgn/K2, characterized by a conservative D57E substitution, exhibits weak binding toward 6AHA ($K_a \sim 2.5$ mM^{-1}) while K3, with a Lys substituting for Asp[57], predictably does not measurably interact with this ligand (Marti *et al.*, 1994). The different affinities toward ω-amino acids exhibited by these kringles indicate that an aromatic pocket and integrity of the Asp[55] + Asp[57](Glu[57]) anionic locus are mandatory for ligand binding while a variable configuration of cationic sites, variously contributed by residues 34, 36, 69, and 71, generates a distributed field of positive electrostatic potential which stabilizes the binding and contributes selectivity to the interaction.

Conspiring against a significant ω-amino acid binding affinity for the tPA/K1 homolog are (a) location of a basic residue (Arg[56]) between the key acidic Asp[55] and Asp[57] anionic centers and (b) lack of an aromatic residue at site 72. Thus, the tPA/K1 domain is expected to exhibit only marginal lysine-binding capability. Indeed, a calorimetric characterization of tPA/K1 in the presence of 6AHA (De Serrano *et al.*, 1992) has shown that, although measurable,

the interaction is extremely weak ($K_a < 0.01$ mM^{-1}).

Overall, the excellent correlation between amplitudes of ligand-induced resonance shifts (Figures 4–7) and the intensity of the intermolecular NOEs (Figures 8 and 9) affords strong evidence that the former reflect mostly perturbations of the *local* magnetic environment of the affected atoms rather than remote structural rearrangements. This fits the paradigm that ligand binding to kringles involves only minor conformational adjustments (Llinás *et al.*, 1985) or, as stated by Tulinsky and co-workers, that *the lysine-binding site appears to be preformed* (Wu *et al.*, 1991).

REFERENCES

Brünger, A. T. (1988) *X-PLOR Version 1.5 User Manual,* Yale University Press, New Haven, CT.

Byeon, I.-J. L., & Llinás, M. (1991) *J. Mol. Biol. 222,* 1035–1051.

Byeon, I.-J. L., Kelley, R. F., & Llinás, M. (1989) *Biochemistry 28,* 9350–9360.

Byeon, I.-J. L., Kelley, R. F., & Llinás, M. (1991) *Eur. J. Biochem. 197,* 155–165.

Cleary, S., Mulkerrin, M. G., & Kelley, R. F. (1989) *Biochemistry 28,* 1884–1891.

Cox, M., Schaller, J., Boelens, R., Kaptein, R., Rickli, E., & Llinás, M (1994) *Chem. Phys. Lipids 67,* 43–58.

De Marco, A. (1977) *J. Magn. Reson. 26,* 527–528.

De Marco, A., Laursen, R. A., & Llinás, M. (1986) *Arch. Biochem. Biophys. 244,* 727–741.

De Marco, A., Petros, A. M., Laursen, R. A., & Llinás, M. (1987) *Eur. Biophys. J. 14,* 359–368.

De Serrano, V. S., & Castellino, F. J. (1992a) *Biochemistry 31,* 3326–3335.

De Serrano, V. S., & Castellino, F. J. (1992b) *Biochemistry 31,* 11698–11706.

De Serrano, V. S., & Castellino, F. J. (1993) *Biochemistry 32,* 3540–3548.

De Serrano, V. S., & Castellino, F. J. (1994a) *Biochemistry 33,* 1340–1344.

De Serrano, V. S., & Castellino, F. J. (1994b) *Biochemistry 33,* 3509–3514.

De Serrano, V. S., Menhart, N., & Castellino, F. J. (1992) *Arch. Biochem. Biophys. 294,* 282–290.

de Vos, A. M., Ultsch, M. H., Kelley, R. F., Padmanabhan, K., Tulinsky, A., Westbrook, M. L., & Kossiakoff, A. A. (1992) *Biochemistry 31,* 270–279.

Gething, M.-J., Adler, B., Boose, J.-A., Gerard, R. D., Madison, E. L., McGookey, D., Meidell, R. S., Roman, L. M., & Sambrook, J. (1988) *EMBO J. 7,* 2731–2740.

Hochschwender, S. M., & Laursen, R. A. (1981) *J. Biol. Chem. 256,* 11172–11176.

Hochschwender, S. M., Laursen, R. A., De Marco, A., & Llinás, M. (1983) *Arch. Biochem. Biophys. 223,* 58–67.

Horrevoets, A. J. G., Smilde, A., de Vries, C., & Pannekoek, H. (1994) *J. Biol. Chem. 269,* 12639–12644.

Kanyo, Z. F., & Christianson, Z. F. (1991) *J. Biol. Chem. 266,* 4264–4268.

Kelley, R. F., de Vos, A. M., & Cleary, S. (1991) *Proteins: Struct., Funct., Genet. 11,* 35–44.

Kohnert, U., Rudolph, R., Verheijen, J. H., Weening-Verhoeff, E. J. D., Stern, A., Opitz, U., Martin, U., Lill, H., Prinz, H., Lechner, M., Kresse, G.-B., Buckel, P., & Fisher, S. (1992) *Protein Eng. 5,* 93–100.

Lerch, P. G., & Rickli, E. E. (1980) *Biochim. Biophys. Acta 625,* 374–378.

Lerch, P. G., Rickli, E. E., Lergier, W., & Gillessen, D. (1980) *Eur. J. Biochem. 107,* 7–13.

Llinás, M., De Marco, A., Hochschwender, S. M., & Laursen, R. A. (1983) *Eur. J. Biochem. 135,* 379–391.

Llinás, M., Motta, A., De Marco, A., & Laursen, R. A. (1985) *J. Biosci. 8,* 121–139.

Markus, G., Camiolo, S. M., Sottrup-Jensen, L., & Magnusson, S. (1981) *Progr. Fibrinolysis 5,* 125–128.

Markward, F. (1978) in *Fibrinolytics and Antifibrinolytics* (Markward, F., Ed.) pp 511–577, Springer-Verlag, Berlin.

Marti, D., Schaller, J., Ochensberger, B., & Rickli, E. E. (1994) *Eur. J. Biochem. 219,* 455–462.

Menhart, N., Sehl, L. C., Kelley, R. F., & Castellino, F. J. (1991) *Biochemistry 30,* 1948–1957.

Menhart, N., McCance, S. G., Sehl, L. C., & Castellino, F. J. (1993) *Biochemistry 32,* 8799–8806.

Motta, A., Laursen, R. A., Llinás, M., Tulinsky, A., & Park, C. H. (1987) *Biochemistry 26,* 3827–3836.

Mulichak, A. M., Tulinsky, A., & Ravichandran, K. G. (1991) *Biochemistry 30,* 10576–10588.

Nielsen, P. R., Einer-Jensen, K., Holtet, T. L., Andersen, B. D., Poulsen, F. M., & Thøgersen, H. Chr. (1993) *Biochemistry 32,* 13019–13025.

Pannekoek, H., Lijnen, H. R., & Loskutoff, D. J. (1990) *Thromb. Haemostasis 64,* 600–603.

Petros, M. A., Ramesh, V., & Llinás, M. (1989) *Biochemistry 28,* 1368–1376.

Rajan, N. (1987) Doctoral Dissertation, Boston University, Boston, MA.

Ramesh, V., Petros, A. M., Llinás, M., Tulinsky, A., & Park, C. H. (1987) *J. Mol. Biol. 198,* 481–498.

Ramesh, V., Laursen, R. A., & Llinás, M. (1989) in Second International Workshop on the Molecular and Cellular Biology of Plasminogen Activation, Brookhaven National Laboratory, Long Island, NY, Abstract, pp 54–55.

Rejante, M. R. (1992) Doctoral Dissertation, Carnegie Mellon University, Pittsburgh, PA.

Rejante, M. R., & Llinás, M. (1994) *Eur. J. Biochem. 31,* 939–946.

Rejante, M., Elliott, B. W., & Llinás, M. (1991a) *Fibrinolysis 5,* 87–92.

Rejante, M. R., Byeon, I.-J. L., & Llinás, M. (1991b) *Biochemistry 30,* 11081–11092.

Skoza, L., Tse, A. O., Semar, M., & Johnson, A. J. (1968) *Ann. N.Y. Acad. Sci. 146,* 659–672.

Sneddon, S. F. (1990) *MolX: A Series of General Purpose Molecular Graphics Programs* (*Version 17*), Carnegie Mellon University, Pittsburgh, PA.

Thewes, T., Ramesh, V., Simplaceanu, E. L., & Llinás, M. (1987) *Biochim. Biophys. Acta 912,* 254–269.

Thewes, T., Constantine, K., Byeon, I.-J. L., & Llinás, M. (1990) *J. Biol. Chem. 265,* 3906–3915.

Trexler, M., Váli, Z., & Patthy, L. (1982) *J. Biol. Chem. 257,* 7401–7406.

Tulinsky, A., Park, C. H., Mao, B., & Llinás, M. (1988) *Proteins: Struct., Funct., Genet. 3,* 85–96.

Váli, Z., & Patthy, L. (1984) *J. Biol. Chem. 259,* 13690–13694.

Van Zonneveld, A.-J., Veerman, H., & Pannekoek, H. (1986a) *J. Biol. Chem. 261,* 14214–14218.

Van Zonneveld, A.-J., Veerman, H., & Pannekoek, H. (1986b) *Proc. Natl. Acad. Sci. U.S.A. 83,* 4670–4674.

Verheijen, J. H., Caspers, M. P. M., Chang, G. T. G., de Munk, G. A. W., Pouwels, P. H., & Enger-Valk, B. E. (1986) *EMBO J. 5,* 3525–3530.

Watt, K. W. K., Takagi, T., & Doolittle, R. F. (1979) *Biochemistry 18,* 68–76.

Wider, A., Macura, S., Kumar, A., Ernst, R. R., & Wüthrich, K. (1984) *J. Magn. Reson. 56,* 207–234.

Wiman, B. (1973) *Eur. J. Biochem. 39,* 1–9.

Wiman, B., & Wallén, P. (1975) *Eur. J. Biochem. 50,* 489–494.

Winn, E. S., Hu, S.-P., Hochschwender, S. M., & Laursen, R. A. (1980) *Eur. J. Biochem. 104,* 579–586.

Wu, T.-P., Padmanabhan, K., Tulinsky, A., & Mulichak, A. M. (1991) *Biochemistry 30,* 10589–10594.

BI941607T